

# Gyrokinetic Simulations of Temperature Gradient Instability in the RFP

V. Tangri<sup>1</sup>, P.W. Terry<sup>1</sup>, R.E. Waltz<sup>2</sup>, and J.S Sarff<sup>1</sup>

1) Department of Physics, University of Wisconsin-Madison, Madison, Wisconsin 53706

2) General Atomics, San Diego, California

e-mail contact of main author: [varun.tangri@gmail.com](mailto:varun.tangri@gmail.com)

**Abstract:** Electrostatic turbulence and transport can dominate reversed field pinch (RFP) confinement when transport from global-scale magnetic fluctuations is reduced by profile control and quasi-single helicity states. Ion and electron temperature gradient (ITG and ETG) turbulence and trapped electron mode (TEM) turbulence are examined in the RFP by adapting the gyrokinetic code GYRO to RFP equilibria. Solution of the Grad Shafranov equation yields toroidal generalizations of the cylindrical Bessel Function model. These are used to study instability for comparable toroidal and poloidal magnetic fields, and with the ultra low safety factor values of the RFP. RFP equilibrium parameters of importance for ITG turbulence, like magnetic shear and safety factor, are not independent and must be varied consistent with their dependence on radial position and pinch parameter. ITG modes are unstable in the RFP. Instability is enabled by the everywhere bad curvature of the poloidal magnetic field. There is no ballooning at the outside midplane. Parallel streaming is important but not enough to produce slab-like eigenmode structure in GYRO. The instability threshold in temperature gradient scale length, normalized to minor radius is comparable to the tokamak threshold scale length, normalized to major radius. This makes the critical gradient in the RFP higher by the aspect ratio. For wavelengths smaller than the sound gyroradius, nonadiabatic electron physics yields instability related to TEM and ETG. Nonlinear simulations indicate a Dimits shift as in tokamaks.

## 1. Introduction

Current profile control techniques [1] and quasi-single helicity states at high plasma current [2] have yielded reversed field pinch (RFP) plasmas with greatly reduced stochastic magnetic transport from global tearing modes. When global tearing modes are controlled, transport from small-scale electrostatic and electromagnetic fluctuations becomes important and can govern confinement, as in the tokamak. However, unlike the tokamak, it is not known what small-scale fluctuations are responsible for confinement degradation. Many types of fluctuations familiar from other toroidal configurations are rendered stable or only feebly unstable by the strong magnetic shear of the RFP [3] – [4]. However, much of the work that established the strong stabilizing influence of shear was based on reduced models. With the emergence of comprehensive models for toroidal geometries, and given the importance of small-scale electrostatic and electromagnetic fluctuations in RFP plasmas when magnetic turbulence is reduced, it becomes crucial to develop comprehensive toroidal models of gyroradius-scale turbulence in the RFP. Computational studies can then be carried out to understand the physics of these fluctuations and assess techniques for their control.

We describe a study of ion temperature gradient (ITG) instability and drift instabilities associated with nonadiabatic electrons in the RFP using the gyrokinetic solver GYRO [5]. ITG turbulence is of central interest because it remains unstable even for the large magnetic shear of the RFP. Moreover, pulsed poloidal current drive (PPCD) yields peaked temperature profiles with flat density profiles, giving large values of  $\eta_i = L_n/L_T$  and therefore providing a strong drive. GYRO was developed for tokamak equilibria, which among other properties, have toroidal fields that significantly exceed poloidal fields, safety factor values  $q$  that are order unity and larger, and toroidal flux that is a single-valued function of radius. We describe here reconfiguration of GYRO to accommodate the RFP equilibrium so that the code handles toroidal and poloidal fields of arbitrary magnitude in toroidal geometry, including the ultra low  $q$  values of the RFP. Part of the reconfiguration is the development of properly ordered, *toroidal* equilibrium approximations of the Grad Shafranov equation that

have the simplicity and utility of the so-called  $s$ - $\alpha$  tokamak equilibrium model [6] or the strictly cylindrical Bessel function model [7] of RFP equilibria. Properly ordered toroidal RFP equilibria are desirable for both physics understanding and validation work.

Based on simulations with reconfigured GYRO, we find that the ITG mode can be unstable in the RFP, particularly for magnetic equilibria attained with current profile control. The mode is driven by the curvature drift resonance but does not balloon significantly when the poloidal field, with its everywhere bad curvature, is dominant. This occurs in the outer parts of the discharge where the driving gradient is strongest, and when the pinch parameter  $\Theta$  is large, as occurs in PPCD. These changes affect ITG stability, mode structure, turbulence and transport and are the subject of qualification and verification efforts described herein. Future work will pursue validation opportunities. When nonadiabatic electrons are included there is significant new instability at wavenumbers above an inverse ion gyroradius, indicating the importance of electron trapping and electron temperature gradient drive.

## 2. Equilibrium Modeling for Gyrokinetic Computation in the RFP

The Bessel function model, while the standard equilibrium representation of the RFP, is a cylindrical equilibrium. We solve the Grad-Shafranov equation for the RFP and establish a hierarchy of approximate toroidal equilibria for computational studies [8]. In the limit of large aspect ratio ( $\varepsilon \equiv a/R_0 \ll 1$ ), where  $R_0$  is the major radius at the flux surface center, the Grad-Shafranov equation is  $R(\partial/\partial R)[(1/R)\partial\Psi/\partial R] + \partial^2\Psi/\partial Z^2 = -\mu_0 R^2 p' - F dF/d\Psi$ . Here  $R$  and  $Z$  are radial and axial coordinates of a cylindrical coordinate system aligned with the toroidal axis of symmetry,  $RB_\phi = F(\Psi)$ , and  $B_\theta = |\nabla\Psi|/R$ , relating  $F$  and  $\Psi$  to the toroidal and poloidal fields  $B_\phi$  and  $B_\theta$ . We introduce the approximation  $F(\Psi) = \mu(\Psi - \Psi_s)$ , where  $\Psi_s$  is a constant of order  $\varepsilon$  or smaller. This approximation is well satisfied by equilibria in MST [9]. Moreover the poloidal component of the force free condition  $\nabla \times B = \mu B$  yields  $j_\theta = (dF/d\Psi)(B_\theta/\mu_0)$ , which implies  $dF/d\Psi = \mu$ . This approximation for  $F$  is substituted into the Grad-Shafranov equation. The average poloidal beta is assumed to be of order  $\varepsilon^2$ , allowing the neglect of the term  $dp/d\Psi$ . The resulting equation is expanded in powers of  $\varepsilon$  and solved order by order up to  $O(\varepsilon)$ . Constants of integration are chosen to satisfy wall boundary conditions. Assuming shifted circular flux surfaces the solution up to this order depends on only two parameters,  $\mu = 2\Theta/a$  and  $r/a$ , where  $\Theta = \langle B_\theta \rangle^{wall} / \langle B_\theta \rangle^{vol}$  is the RFP pinch parameter. The solution is

$$\Psi(r/a) = \frac{aB_0}{2\Theta} [J_0(ar\Theta/a) - J_0(2\Theta)],$$

$$\varepsilon\Delta(r/a) = \frac{a}{4} \left[ \sqrt{\pi} \frac{F_1(2r\Theta/a)}{J_1(2\Theta)} \left(\frac{r}{a}\right)^2 + \frac{2\delta}{\Theta} \right],$$

where  $\delta = -(\pi)^{1/2}(\Theta/2)F_1(2\Theta)/J_1(2\Theta)$  and  $F_1$  is a combination of Bessel functions [8]. The shift  $\Delta$  is different from tokamak equilibrium models in two ways. Its radial variation is not quadratic, and it exists even for zero beta.

From this solution the toroidal and poloidal fields are given by

$$B_\phi = \frac{B_0 J_0(2r\Theta/a)}{[1 + \varepsilon(r/a)\cos\theta]}, \quad (1)$$

$$B_\theta = \frac{B_0 J_1(2r\Theta/a)}{\left[1 + \varepsilon \left(\frac{r}{r + \Delta'}\right) \cos\theta\right]}, \quad (2)$$

where  $\Delta' = (\partial/\partial r)\Delta(r/a)$  and  $\theta$  is the poloidal angle on the flux surface measured from the outboard midplane. When the gradient in the poloidal beta is large the flux surface shift  $\Delta'$  is important. Otherwise, the shift can be neglected, yielding

$$B_\phi = \frac{B_0 J_0(2r\Theta/a)}{\left[1 + (r/R_0) \cos\theta\right]}, \quad (3)$$

$$B_\theta = \frac{B_0 J_1(2r\Theta/a)}{\left[1 + (r/R_0) \cos\theta\right]}. \quad (4)$$

Note that this result corresponds to a generalization of the Bessel function model to include the factor  $(1/R)$  of toroidal geometry. The factor applies to both components of the field. We call this equilibrium the toroidal Bessel function model (TBFM). The equilibria of Eqs. (1)-(2) or (3)-(4) can be used as reduced equilibria in GYRO for assessing scalings and trends of instabilities and turbulence. These replace the  $s$ - $\alpha$  equilibrium, which is not appropriate when the poloidal field becomes large. For RFP discharges with  $\Theta > 3$ , the approximations made in deriving Eqs. (1) and (2) break down. In such cases local Miller equilibria could, in principle, be fitted to experimental RFP equilibria using the full available parameter set of the Miller equilibrium embedded in GYRO to capture the shape of the flux surfaces.

In the RFP both the toroidal and poloidal fields are constrained by the internal physics of relaxation. Consequently parameters on which ITG instability is sensitive, and which are treated as independent in tokamak modeling, cannot be varied independently in the RFP. Magnetic shear  $s$  and  $q$ , which affect stability through the magnetic drifts, are functions of

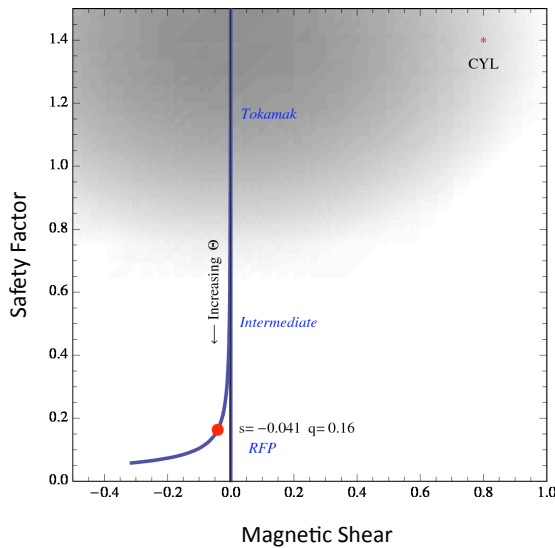


Fig. 1. Variation of  $q$  and  $s$  with  $\Theta$

The magnetic shear changes little at first and then drifts to negative values. The red point is  $\Theta = 2$  and corresponds to a typical RFP equilibrium with  $q = 0.16$  and  $s = -0.041$ . For reference, the point marked by a '\*' and labeled 'CYL' is the tokamak cyclone base case

radial position and pinch parameter  $\Theta$ . For the TBFM whose fields are given in Eqs. (3) and (4),  $q = (\varepsilon r/a) J_0(2\Theta r/a) / J_1(2\Theta r/a)$ , and  $s = 2 - 2q\Theta/\varepsilon - 2r^2 \varepsilon \Theta / qa^2$ . These approximations are valid if  $\Theta$  is not too large, a condition met in standard discharges. In PPCD discharges  $\Theta$  is larger and the equilibrium must be taken from experiment. The dependence of  $q$  and  $s$  on  $\Theta$  is illustrated in Fig. 1, where  $\Theta$  is varied for fixed  $r/a = 0.1$ . Magnetic shear and safety factor are constrained to lie on the curved line. The upper part of the curve corresponds to small  $\Theta$ , and the field is tokamak like with  $B_\phi \gg B_\theta$  and weak shear. As  $\Theta$  increases, increasing poloidal field drops the safety factor to small values.

[10]. For larger  $r/a$  the curve is displaced further to the left, giving more negative values of magnetic shear for a given  $\Theta$ .

### 3. Linear Instability Properties

RFP discharges have  $q \ll 1$  and magnetic shear  $s < 0$ , wholly outside the parameter space of tokamak operation. It is therefore essential to perform verification of GYRO with the RFP equilibrium modifications. At sufficiently small  $\Theta$  and  $r$ ,  $B_\phi$  exceeds  $B_\theta$ , as in a tokamak. In this case an RFP equilibrium such as the TBFM and a standard Miller tokamak equilibrium [11] converge. Benchmarking with tokamak runs verifies ITG growth rate calculations for RFP equilibrium modifications. As  $\Theta$  and  $r$  increase,  $B_\theta$  becomes larger than  $B_\phi$ . Because the ITG instability is sensitive to the curvature drift resonance this change in magnetic field configuration leads to changes in the growth rate. This is illustrated in Fig. 2, which shows the real frequency and growth rate at various radial positions for  $\Theta = 1.35$ . At small  $r$  the Miller and TBFM results closely agree. At larger values of  $r$  the growth rates are different, with the TBFM yielding lower growth rates for higher values of  $k_\theta \rho_s$ . The mode structure at higher values of  $r$  does not balloon at the outside midplane, rather its extent along the field line greatly increases. As a result, converged growth rates require much larger parallel resolution than for the tokamak, and much greater temporal resolution. The growth rate remains strongly dependent on the curvature drift, but it is the curvature drift of the poloidal

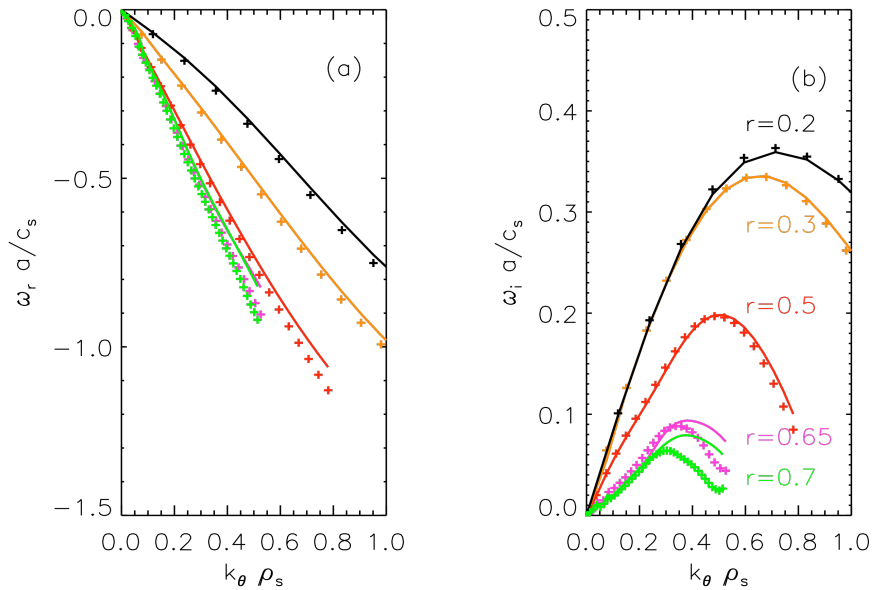


Fig. 2. Normalized real frequency (a) and growth rate (b) as functions of poloidal wavenumber for a variety of radial positions. Solid lines indicate a tokamak equilibrium provided by the Miller model and the '+' symbols indicate the TBFM.

field, indicating that drive is enabled by the everywhere-bad curvature of the poloidal field. The parallel streaming term  $k_\parallel v_\parallel$  is large in the RFP, but not enough to force a slab-like mode structure. Nonetheless the term remains essential for quantitatively correct predictions of the growth rate. The ITG instability for  $q \ll 1$  and  $s < 0$  has shear scaling like that of tokamak regimes: the growth first increases with more negative magnetic shear, and then decreases, consistent with the importance of the curvature drift resonance over the parallel streaming resonance. The scaling of growth rate with temperature ratio  $T_i/T_e$  is also similar to that of the tokamak. The growth rate decreases with increasing  $\Theta$ .

As shown in Fig. 3, variation of the temperature gradient scale length  $L_T$  establishes that for the RFP, the ITG threshold gradient  $L_{Tcrit}$ , normalized to minor radius is comparable in magnitude to the tokamak threshold gradient normalized to the major radius, i.e.,  $a/L_{Tcrit}|_{RFP} \approx R/L_{Tcrit}|_{TOK}$ . Hence the critical gradient is order  $R/a$  higher in the RFP. This difference is

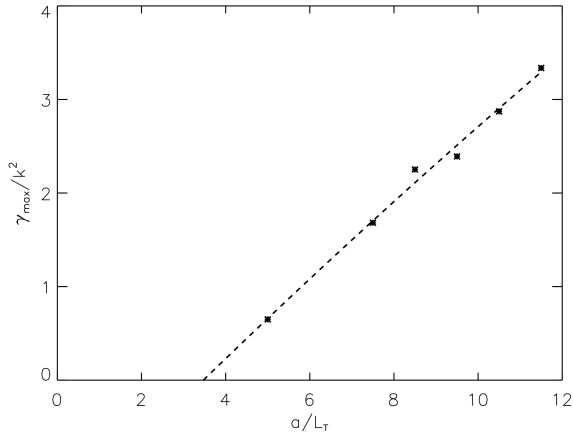


Fig. 3. Growth rate as a function of  $a/L_T$

consistent with the growth rate dependence on poloidal curvature in the RFP, the unavailability of ballooning to magnify the destabilizing effect of bad curvature, and the fact that magnetic shear is stronger in the RFP than in the tokamak by  $R/a$ . These observations suggest that there may be a subdominant slab-like branch that could become dominant for certain parameters. They also indicate that ITG may remain active at smaller radial locations in the RFP than in the tokamak due to the increasing importance of toroidal field. The results of these studies are at variance with analytical calculations [12], which have used invalid simplifying assumptions for the kinetic operator. Indeed the importance of both the Landau and curvature drift resonances in the kinetic operator make the RFP a more stringent test bed for validation of the gyrokinetic model than the tokamak, and point to a significant validation opportunity.

#### 4. Microturbulence Physics Studies for the RFP

Non adiabatic electrons have been included in linear stability calculations, as illustrated in Fig. 4, which shows the real frequency and growth rate as a function of  $k$  for a calculation

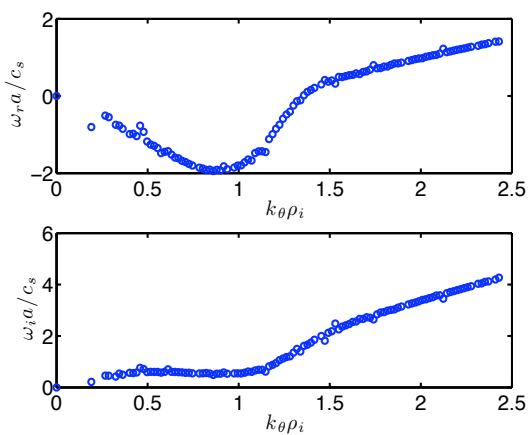


Fig. 4. Real frequency and growth rate as function of  $k$  with non adiabatic electrons.

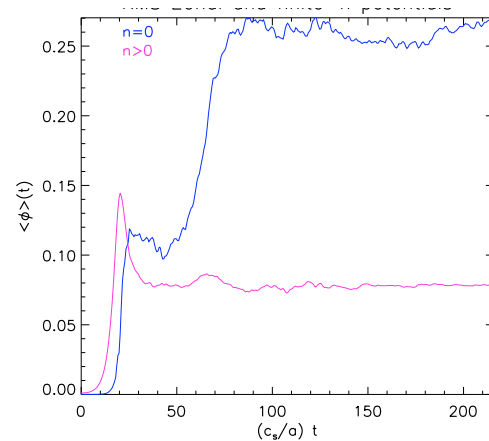


Fig. 5. Time histories of zonal flow and finite  $n$  potentials

with zero beta. Below  $k\rho_s = 0.8$ , the growth rate is the same with or without nonadiabatic electrons. Above this value the growth rate increases sharply when nonadiabatic electrons are included; otherwise it decreases. The mode frequency changes from the ion to the electron diamagnetic direction as the wavenumber increases into the range of this new instability. Electrostatic mode structures in the high  $k$  region have even parity along the field line. In tokamaks the new branch is the trapped electron mode (TEM) at intermediate  $k$  and

the electron temperature gradient mode at higher  $k$ . The mode structure and frequency suggest that TEM operates in the RFP, a fact that has not been verified previously. It should be noted that there are significant numbers of trapped electrons in the RFP, from both toroidal and poloidal fields, as indicated by the TBFM, Eqs. (3) and (4).

Flux tube simulations of saturated ITG turbulence have been performed for a range of values of the temperature gradient scale length. The heat diffusivity shows a Dimits shift, increasing weakly with  $a/L_T$  right above the threshold, and then increasing more sharply further above the threshold. This behavior is related to zonal flows. Figure 5 shows time histories of the electrostatic potential for  $n = 0$  and finite  $n$  components. There is a significant zonal flow. It should be noted that in the RFP edge, where the field is predominantly poloidal, the zonal flow is toroidal. Recent gyrokinetic studies of ITG turbulence in tokamaks have shown that the turbulence is saturated by stable eigenmodes that damp energy injected by the instability in the same wavenumber range as the instability [13]. Zonal flows provide an efficient energy transfer channel from the instability to the stable eigenmodes [14]. When this channel is artificially suppressed, energy flows to the damped eigenmodes through less efficient channels, which require larger amplitudes. This process is expected to apply to the RFP and will be studied in the future. The possible role of ITG turbulence in the spontaneous rotation of RFP plasmas will also be investigated.

## 5. Conclusions

The stability and fluctuation properties of temperature gradient driven drift waves, including ITG, TEM and ETG, have been studied for RFP plasmas using gyrokinetics. The Grad-Shafranov equation has been solved under an aspect ratio expansion, yielding toroidal equilibrium approximations, including a toroidal generalization of the Bessel function model of RFP equilibria. These equilibria are parameterized by the radius and pinch parameter, and indicate that quantities such as magnetic shear and safety factor are not independent. The toroidal equilibria derived are used in GYRO to study microinstability and turbulence in the ultra low  $q$ , negative magnetic shear environment of the RFP. The ITG mode is unstable in the RFP, with a threshold measured in  $a/L_T$  that is comparable to the tokamak threshold measured in  $R/L_T$ . Growth rates decrease with the pinch parameter. The instability is sensitive to the curvature of the poloidal field and shows little tendency to balloon. Extended mode structure along the field line requires significantly larger parallel resolution than that of the tokamak. The toroidal equilibrium admits significant trapped particles and nonadiabatic electrons lead to trapped electron instability above  $k\rho_s = 0.8$ .

Work supported by USDOE under the grant DE-FG02-85ER53212.

- [1] J.S. Sarff, S.A. Hokin, H. Ji, S.C. Prager, and C.R. Sovinec, Phys. Rev. Lett. **72**, 3670 (1994).
- [2] R. Lorenzini, et al., Nature Physics **5**, 570 (2009).
- [3] N.T. Gladd and C.S. Liu, Phys. Fluids **22**, 1289 (1979).
- [4] G.G. Craddock, P.W. Terry, and K.L. Sidikman, Sherwood Theory Conference (Williamsburg, 1990, paper 3C37).
- [5] J. Candy and R.E. Waltz, J. Comput. Phys. **186**, 545 (2003).
- [6] J.M. Greene and M.S. Chance, Nucl. Fusion **21**, 453 (1981).
- [7] J.B. Taylor, Phys. Rev. Lett. **33**, 1139 (1974).
- [8] V. Tangri, P.W. Terry and R.E. Waltz, submitted to Phys. Plasmas.
- [9] J. Anderson, C. Forest, T. Biewer, J. Sarff, and J. Wright, Nucl. Fusion **44**, 162 (2004).
- [10] A.M. Dimits, et al. Physics of Plasmas **7**, 969 (2000).

- [11] R.L. Miller, M.S. Chu, J.M. Greene, Y.R. Lin-Lin, and R.E. Waltz, *Phys. Plasmas* **5**, 973 (1998).
- [12] S.C. Guo, R. Paccagnella, and F. Romanelli, *Phys. Plasmas* **1**, 2741 (1994).
- [13] D.R. Hatch, et al., submitted.
- [14] K. Makwana, P.W. Terry, J.-H. Kim, and D.R. Hatch, APS DPP 2010.